



**ITTC – Recommended  
Procedures and Guidelines**

**7.5-03  
04 - 01**  
Page 1 of 17

**Guideline on Use of RANS Tools for  
Manoeuvring Prediction**

Effective Date  
2017

Revision  
01

**ITTC Quality System Manual**

**Recommended Procedures and Guidelines**

**Guideline**

**Guideline on Use of RANS Tools for Manoeuvring Prediction**

7.5	Process Control
7.5-03	CFD
7.5-03-04	Manoeuvrability
7.5-03-04-01	Guideline on Use of RANS Tools for Manoeuvring Prediction

Prepared by	Approved
Manoeuvring Committee of the 28 <sup>th</sup> ITTC	28 <sup>th</sup> ITTC 2017
Date 01/2017	Date 09/2017

## Table of Contents

<b>1. PURPOSE OF GUIDELINE .....</b>	<b>3</b>	2.2.1 Motion equations of the ship.....	8
<b>2. SIMULATION APPROACH .....</b>	<b>3</b>	2.2.2 Coupling of ship motions & flow.	9
<b>2.1 General Considerations.....</b>	<b>3</b>	<b>2.3 Simulation of Forced Motions .....</b>	<b>10</b>
2.1.1 Scale .....	3	2.3.1 Forced ship motions .....	10
2.1.2 Governing Equations of the Fluid	3	2.3.2 Analysis of predicted forces.....	10
2.1.3 Turbulence Model .....	4	<b>3. SIGNIFICANT PARAMETERS .....</b>	<b>10</b>
2.1.4 Propulsion and Steering Model ...	4	<b>4. EXAMPLES.....</b>	<b>11</b>
2.1.5 Computational Grid.....	5	<b>4.1 Direct Manoeuvring Simulation.....</b>	<b>11</b>
2.1.6 Coordinate Frame .....	6	<b>4.2 Simulation Based on Derivatives....</b>	<b>11</b>
2.1.7 Boundary Conditions.....	6	<b>5. REFERENCES .....</b>	<b>16</b>
2.1.8 Free surface treatment .....	8		
2.1.9 Flow current .....	8		
<b>2.2 Direct Manoeuvring Simulation.....</b>	<b>8</b>		

## Use of RANS Tools for Manoeuvring Prediction

### 1. PURPOSE OF GUIDELINE

RANS tools, i.e. numerical methods for solving the Reynolds Averaged Navier Stokes equations for viscous turbulent flows, can be applied to predict the manoeuvring behaviour of a vessel. This is achieved either in a direct way, using the considered RANS code for predicting the trajectory and, more in general, the 6 Degrees of Freedom (DOF) motion due to the movement of an appendage such as the rudder, or using it to calculate the hydrodynamic forces and moments acting on the ship or ship model during forced motions. The latter results can be used to determine manoeuvring derivatives for manoeuvring predictions.

A description of different techniques is presented from the practical point of view, together with recommended practices to obtain feasible manoeuvring prediction results. The numerical techniques used to discretise the involved partial differential equations, e.g. finite difference method or finite volume method, to model the turbulence of the flow and to generate grids have been described in many publications (e.g. Anderson et al., 1984; Blazek, 2001; Ferziger and Peric, 2002; Hirsh, 1988; Wilcox, 1993).

The present guideline is dedicated to surface ships in mainly unrestricted waters, where usually only four degrees of freedom (surge, sway, yaw, roll) are relevant for manoeuvring. In revision 01 some considerations were added for shallow or restricted water conditions.

### 2. SIMULATION APPROACH

#### 2.1 General Considerations

##### 2.1.1 Scale

In principle RANS simulations can be done for the full scale ship, avoiding any scale effect. In practice however, most simulations are performed for the ship model rather than the full scale ship because computations for Reynolds numbers of the order  $10^9$  are not fully validated yet and yield much more numerical difficulties than for Reynolds number at model scale, being 2 orders of magnitude smaller. In addition, prediction results for the model can be judged as a whole by comparing them with the results of a few selected free model tests. This “hybrid” prediction procedure seems especially attractive for towing tanks.

##### 2.1.2 Governing Equations of the Fluid

The Navier-Stokes (NS) equations and the continuity equation describe the conservation of momentum and mass in a viscous turbulent incompressible flow and are best suitable to describe the flow around a ship. In order to work with mean values of all flow variables (e.g. velocities, pressure) instead of instantaneous values, the RANS equations are obtained by averaging the NS equations. This averaging can be seen as time averaging in case of a steady mean flow, but has to be understood as ensemble averaging in case of an unsteady mean flow (e.g. Wilcox, 1993; Cebeci et al., 2005). As a result of the averaging, the RANS equations contain some new unknown terms representing the effect of the turbulence on the flow. In order to

solve the set of conservation equations, these terms are approximated by a turbulence model. The reason for doing so is that if not, the required space and time resolution for solving the NS equations directly would be impracticable (probably still in the next decades) for a turbulent ship flow.

### 2.1.3 Turbulence Model

Any turbulence model used by usual RANS applications can also be used for manoeuvring tasks. The most popular models are the family of  $k-\varepsilon/k-\omega$  SST models (Launder and Spalding, 1974; Wilcox, 1993; Menter et al., 2003) and several variants primarily using wall functions, which allow a significant more coarse resolution of near wall regions.

Other models like explicit algebraic stress models, detached eddy simulation (DES) models or one equation models are also applied for manoeuvring computations (SIMMAN 2014).

When looking for prediction of complex flow phenomena however, e.g. detailed flow separation, none of the turbulence models can accurately predict all aspects of the flow with current grids and solvers (Abdel-Maksoud et. al 2015).

Results presented at the CFD Workshops held in Gothenburg (2010) and Tokyo (2015) have shown a strong dependency for both the resistance and the velocity field on the turbulent model, however, the experience from published results and workshops shows that the dependence of the turbulence model on side force and yaw moment, i.e. the forces which are most significant for manoeuvring, is less significant (Abdel-Maksoud et al., 2015). One possible reason is that these hydrodynamic forces are certainly viscosity dependent but primarily dominated by pressure. In fact, satisfactory results can be achieved even using wall functions as

they do not deteriorate the quality of the predictions to the same extent as when predicting resistance.

### 2.1.4 Propulsion and Steering Model

Disregarding cases where RANS tools are used for predicting forces on the bare hull only, e.g. to determine coefficients for hull forces in a modular mathematical model, the appendages have to be taken into account for manoeuvring tasks. Inclusion of rudders and even bilge keels has become usual in RANS applications. This complicates the grid generation and probably also some flow aspect which can lead to increased convergence difficulties, but does not really represent a problem.

The main issue is how to treat the propeller(s), which is crucial for simulating the rudder inflow correctly when rudders are placed behind propellers. Taking the real geometry of the propeller into account and considering the rotating propeller during the RANS simulation is possible (Carrica and Stern, 2008) but extremely time consuming. Thus, body forces, which are added to the right hand sides of the RANS equations, are frequently used to approximate the effect of the propeller on the flow. These forces are distributed over the grid region corresponding to the spatial position of the propeller and are calculated so that they yield the propeller thrust and torque.

Body force models, mostly based on potential flow codes like vortex-lattice or panel methods, are often used for approximating the propeller effect including slip stream and swirl, which may also influence aspects of the flow like rudder stall angle, risk of cavitation, etc. The body force distribution inside the propeller region may be calculated in every new time step or in some larger time intervals, based on the current propeller inflow obtained during the RANS simulation and on the propeller rpm. This

can be done either interactively, running the used potential code each time again, or determining the forces in grid cells within the propeller region from a data base calculated beforehand for the considered propeller. Fig.1 shows the cylindrical body force region (rectangle) and the effect of the body forces on the axial velocity in the longitudinal central plane.

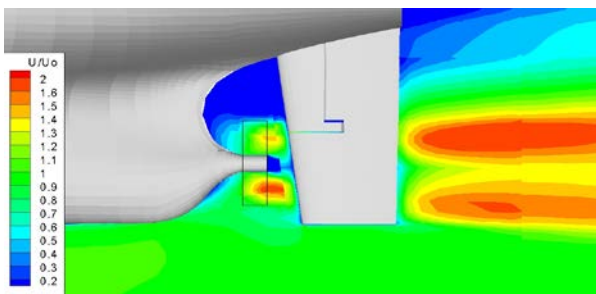


Fig.1 Body force region and effect on the flow

The choice of the propulsion point, corresponding to the full scale or to the model scale, should be decided following similar criteria as for model tests (see procedure 7.5-02-06-02). A way for determining the correct propeller rpm before starting the manoeuvre simulation is to calculate the flow for the steady straight ahead motion of the ship at the given approach speed for different rpm's and to determine the one which makes the total longitudinal force equal to the desired value (e.g. zero or estimated frictional deduction).

A proper strategy for the propeller rpm during the manoeuvre, resembling the real behaviour in full scale where the rpm often varies depending on torque, can also be implemented.

The choice of propeller model can have a significant effect on the manoeuvring simulation results as the body force propeller does not take into account the lateral propeller forces (Hamid et al., 2014; Broglia et al., 2011). Lateral forces should be included to get more accurate results.

### 2.1.5 Computational Grid

Commercial grid generators are widespread, but also open source software is getting more popular recently. Block-structured grids, often including non-matching interfaces, and unstructured grids with several millions cells have become usual for manoeuvring applications.

Contrary to many CFD applications for ship resistance or propulsion, the nature of the problem now requires a grid covering the surroundings at both sides of the ship.

Not only for turning the propeller but also to deflect the rudder within direct manoeuvring simulations, a RANS code with sliding grid or overlapping grid capability is needed (Carrica et al., 2013; Muscari, 2008 and Durante, 2010). In the later case a considerable amount of computational effort is required for transferring flow information from one grid part to the other. Otherwise and whenever possible, the grid is kept unchanged during the computation in order to not deteriorate its quality which directly influences the convergence behaviour and the quality of the results. However, this is obviously not possible in many cases of interest for example when considering squat in shallow water or approaching a quay. In such cases a suitable grid deformation technique can be an alternative to overlapping grids (Ji, 2010).

The grid can be generated in several ways and many different grid topologies can be chosen. The outer boundaries of the grid mostly consist in planes delimiting a box (hexahedron) surrounding the ship. Fig.2 shows a typical configuration for a manoeuvring application for a double body in deep water.

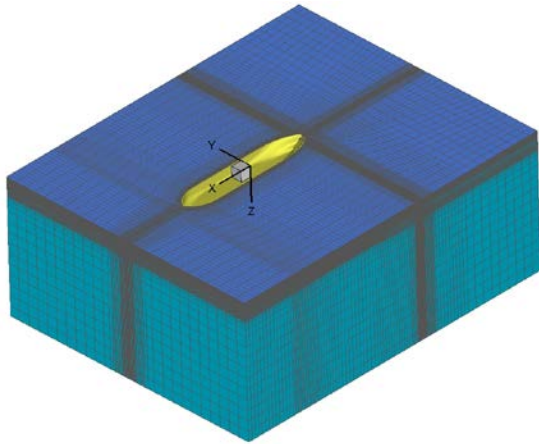


Fig.2 Grid and boundaries of hexahedral computational domain

The grid has to cover the flow domain of interest in such a way that non-physical boundaries (see 2.1.7) are far away of the region of interest, i.e. the ship vicinity. Typical dimensions of a grid are 3-5 ship lengths in longitudinal direction, 2-3 in transverse direction and one length in vertical direction for deep water.

The near wall region has to be meshed so that the requirements of the used turbulence model are fulfilled (e.g. Wilcox, 1993; Menter et al., 2003). In any case, a certain number of grid points within the boundary layer have to be placed dependent on the turbulence model. For the reasons mentioned in subsection 2.1.3 regarding the influence of viscosity on side force and yaw moment, wall functions are often used for manoeuvring cases.

For shallow and restricted water, the grid has to be dense enough to propagate the wave and pressure field and resolve possible boundary layers in the surrounding environment. On vertical walls and bottom surfaces wall functions may be used to avoid large grid densities. The grid size is defined accordingly to the wall function.

In case waves are included in the simulation, the grid size near the free surface should be defined accordingly to the wave length and height.

#### 2.1.6 Coordinate Frame

If the flow computation is made in a ship fixed coordinate frame, i.e. if the conservation of momentum is stated in terms of its components in a ship fixed coordinate system, inertial body forces, e.g. centrifugal and Coriolis forces, have to be added to the RANS equations. These forces are usually treated explicitly during the computation and could affect the stability and convergence of the computation if they are considerably larger than the hydrodynamic forces themselves.

On the other hand, if the flow computation is made in an earth fixed or inertial coordinate frame, no inertial forces have to be added but cell boundary velocities will have to be considered in order to calculate the correct mass and momentum fluxes through the cell sides; see for instance Ferziger and Peric (2002). Both procedures are mathematically equivalent. The numerical advantages of one or the other procedure seem not significant for typical manoeuvring applications.

#### 2.1.7 Boundary Conditions

The boundary conditions (BC) are crucial for the accuracy of the numerical solution. Setting non-physical boundary conditions such as undisturbed flow (Dirichlet) or zero-gradient (Neumann) too close to the ship will affect the results. The way BC are imposed within the numerical technique may change from code to code but does not differ for manoeuvring tasks from other applications. However, during manoeuvring simulations there are often no longer unambiguous inlet or outlet borders of the computational domain but mixed forms.

In unsteady flow cases, the BC may have to be updated in the course of the simulation according to the instantaneous ship motion.

At an “inlet” border for instance, far in front of the ship (e.g.  $1 L_{pp}$ ) the absolute velocity is zero (in absence of current and waves).

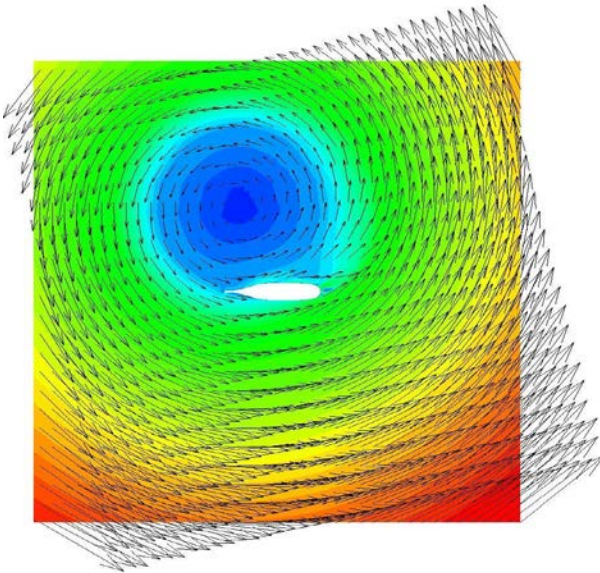


Fig.3 Velocities in horizontal plane around a ship in steady turning to starboard with drift angle  $22^\circ$

Within a ship fixed frame however, inlet velocities are relative velocities and therefore of equal magnitude but opposite sign than the velocity resulting in the considered point of the boundary from the translation and rotation of the ship fixed coordinate system:

$$u_{\text{inlet}} = - ( u - y r )$$

$$v_{\text{inlet}} = - ( v + x r )$$

A pressure BC, either zero pressure for double body flow or undisturbed hydrostatic pressure distribution for free surface flow, has proven to be advantageous for the “outlet” border far behind the ship (e.g.  $2-4 L_{pp}$ ).

At the sides of the computational domain, e.g. placed  $1-2 L_{pp}$  away from the ship, the velocities may also be given, but these borders could also be treated as inlet and outlet boundaries, for instance in case of a steady oblique towing motion at large drift angle.

At rigid walls like the hull, a “no slip” BC is mostly set, ensuring that the fluid particles have the same velocity as the wall. Sometimes however, it is convenient to consider a wall without any friction, a “free slip” wall, for instance to delimit the computational domain. Note that, if planar, such walls behave similar to symmetry planes.

The bottom of the computational domain can be seen as a free slip wall placed far below the ship for deep water (e.g. one  $L_{pp}$ ). Same can be chosen for the top border of the considered hexahedral domain, placed at the waterline in case of double body flow or at some distance (e.g.  $0,1 - 0,3 L_{pp}$ ) above the waterline in case of a free surface flow.

For shallow water the bottom is mostly treated similar to the rigid walls mentioned above, i.e. a no slip BC or a moving no slip BC, depending on the simulation approach, is set to ensure the fluid particles have the same velocity as the bottom.

Note that during manoeuvres often no real inlet and outlet boundaries exist and a border of the computational domain may change its character during the simulation. For these reasons some adapted “mixed” BC taking this feature into account have proven to be very advantageous. Hereby the velocities are given if the flux is directed into the domain only and they are let free otherwise. This has been done at the left, upper and lower lateral borders in the example of Fig.3, while undisturbed pressure was as-

sumed at the right border. The calculated velocity field differs from the undisturbed field in the close vicinity of the ship only.

#### 2.1.8 Free surface treatment

Computations can be performed taking the water free surface into account or not. The latter approach is reasonable for a slow ship in deep water and requires significantly less computational effort (e.g. factor 10). However, even at low Froude numbers, the underwater shape and thus the forces could change significantly if the sinkage and trim of the vessel vary at large drift angle or yaw rate. A way to take such changes into account would be including the free surface and using a 6 DOF motion model (see below) letting the ship free to sink and trim during the simulation.

Including the water free surface however, even having become more standard in the last years, leads not only to more computational time but also to increased numerical difficulties. In particular, reflection of the waves generated by the ship on non-physical or open boundaries (outlet) should be avoided. Among other techniques to avoid such reflections, a strong coarsening of the grid towards the outlet has proven to be very efficient in damping the outgoing waves preventing reflections in a rather rude manner. This procedure however would not be applicable if the considered boundary changes its type (e.g. from outlet to inlet) in the course of the simulated manoeuvre.

#### 2.1.9 Flow current

CFD simulations are usually carried out in uniform current in velocity and direction, which is also the assumption at sea trials. In this case, the current has no influence on the manoeuvring forces or trajectory since motions through water are considered. Consequently, computations can

be performed without current. This is less evident in shallow or confined water as the blockage of the vessel will affect the current flow and the current field will have a boundary layer on the bottom and the banks, yielding a non-uniform current situation. So far non-uniform current has not been given much attention in CFD simulations. For that specific case, an earth fixed reference frame seems to be the easiest choice (see 2.1.6).

## 2.2 Direct Manoeuvring Simulation

Rudder manoeuvres like zigzag tests and turning circle tests are simulated by solving together the motion equations of the ship, considered as a rigid body, and the RANS equations for the fluid. The rudder(s) is (are) turned according to the desired manoeuvre during the simulation. This kind of manoeuvring simulation is extremely time-consuming but, since there is no mathematical model for the hydrodynamic forces involved, in principle easier than by means of manoeuvring derivatives. It will represent the best approach once comprehensively validated.

### 2.2.1 Motion equations of the ship

In order to predict the manoeuvre, the rigid motion equations of the ship in 3-DOF, 4-DOF or even in 6-DOF are numerically integrated in time with a proper discretisation scheme, e.g. Euler implicit, Runge-Kutta, etc. In most applications, provided large accelerations are not expected, the Euler explicit scheme can be used as well. The considered motion parameters should be properly defined by means of an earth-fixed or “inertial” coordinate system, a ship-fixed coordinate system and/or with help of an intermediate or “hybrid” coordinate system to uniquely define angles and translations. The singularity (gimbal lock, typically for  $\cos\theta=0$ ) occurring

when using Euler angles is not relevant for a surface ship.

An example of motion equations in four degrees of freedom (4 DOF) for a free sailing (rigid) ship or model, written in a hybrid coordinate system which follows the ship motions excepting roll, reads:

$$m \left[ \dot{u} - \dot{\psi} v - x_G^* \dot{\psi}^2 + z_G^* (2 \dot{\psi} \dot{\phi} \cos \phi + \ddot{\psi} \sin \phi) \right] = X$$

$$m \left[ \dot{v} + \dot{\psi} u + x_G^* \ddot{\psi} + z_G^* \left( (\dot{\psi}^2 + \dot{\phi}^2) \sin \phi - \ddot{\phi} \cos \phi \right) \right] = Y$$

$$\begin{aligned} & (I_{yy} \sin^2 \phi + I_{zz} \cos^2 \phi) \ddot{\psi} + 2 (I_{yy} - I_{zz}) \dot{\psi} \dot{\phi} \sin \phi \cos \phi \\ & - I_{xz} (\ddot{\phi} \cos \phi - \dot{\phi}^2 \sin \phi) + m x_G^* (\dot{v} + u \dot{\psi}) \\ & + m z_G^* \sin \phi (\dot{u} - v \dot{\psi}) = N \end{aligned}$$

$$\begin{aligned} & I_{xx} \ddot{\phi} - I_{xz} \ddot{\psi} \cos \phi + (I_{zz} - I_{yy}) \dot{\psi}^2 \sin \phi \cos \phi \\ & - m z_G^* \cos \phi (\dot{v} + u \dot{\psi}) = K \end{aligned}$$

The surge and sway velocities  $u$  and  $v$  are the components of the velocity of the chosen ship origin  $O$  in the horizontal longitudinal and transversal directions  $x$  and  $y$  of the hybrid coordinate system, respectively. The Euler angles  $\phi$  and  $\psi$  are the rotations around the  $x$ - and  $z$ -axes respectively and describe the roll and yaw motions of the ship. The dots in the above equations denote time derivatives.  $m$  is the mass of the ship or model and  $x_G^*$  and  $z_G^*$  are the coordinates of the center of gravity  $G$  in the ship fixed system. It is assumed that  $y_G^* = 0$ .  $I_{xx}$ ,  $I_{yy}$ ,  $I_{zz}$  are the moments of inertia about the ship fixed axes through the origin  $O$  and  $I_{xz}$  is the product of inertia. It is assumed that  $I_{xy} = 0$  and  $I_{yz} = 0$  (valid for ships that have a longitudinal plane of symmetry).  $X$  and  $Y$  (longitudinal and side force) are the components in the hybrid system of the external force acting on the ship.  $K$

and  $N$  (roll and yaw moment) are the components in the hybrid system of the moment of the external forces.

Since heave and pitch motions are neglected, the state of movement of the ship is defined by the position of  $O$  (earth fixed coordinates), its velocity vector  $(u, v, 0)$ , the Euler angles  $\phi$ ,  $\psi$  and the angular velocity vector  $(\dot{\phi}, 0, \dot{\psi})$ . The time history of these variables can be obtained by integrating the motion equations in time numerically. For this purpose, the hydrodynamic forces and moments on their right hand sides are needed.

The hydrodynamic forces and moments appearing in the right hand side of the motion equations are calculated in the course of the time integration by simulating the flow at every new time step. Note that even if heave and pitch are not relevant for manoeuvring prediction in unrestricted water, the ship/model should be free to sink and trim during the RANS simulation in order to get the hydrodynamic forces for the most realistic floating condition as possible.

This is easily fulfilled when making simulations with a fully 6-DOF motion model.

Note that it is possible to disable selected motions during the simulations and also to add some external forces, like a frictional deduction force resembling the free model test condition.

## 2.2.2 Coupling of ship motions & flow

The coupling between the ship motions and the flow is crucial for determining the hydrodynamic forces. If only moderate ship accelerations are involved (as usual during manoeuvres) this coupling can easily be implemented in an explicit manner: In every new time step of the simulation the RANS code is used to calculate the forces acting on the ship. Subsequently the

motion equations yield the motion parameters for the next time step. Finally, the boundary conditions and inertial forces (if present) are updated before starting a new time step.

More sophisticated and in general more robust techniques have been recommended, however, at the cost of (significantly) larger computational effort.

### 2.3 Simulation of Forced Motions

Due to the enormous computational effort required for the direct simulation of manoeuvres described above, another strategy has gained popularity instead. It consists in simulating the usual PMM or CPMC tests numerically, solving the RANS equations around the ship or ship model when performing prescribed motions. Compared to direct manoeuvring simulations, this prediction procedure has the same advantages and disadvantages as between free and captive model tests. From the computational point of view however, it is definitively more robust and less time consuming.

The strategy fully resembles the classical, well accepted PMM tests followed by the determination of derivatives and seems already practicable for commercial applications. Nevertheless a mathematical model (e.g. a set of coefficients of Abkowitz type or coefficients of formulae for diverse forces of a modular simulation method) is involved, introducing a further source of uncertainty into the prediction.

#### 2.3.1 Forced ship motions

Motion equations are not solved in this case. Selected motions, e.g. harmonic pure sway, pure yaw, etc, are imposed. There are different ways for imposing the motions. In order to resemble CPMC tests or to reproduce measured motions during free model tests it can be advantageous

to read a file containing the time histories for the motion parameters.

Note that also in this case and disregarding that the ship motion is given, it would be best to let the ship or model free to sink and trim during the RANS simulation. However, contrary to subsection 2.2.1 where the motions are predicted anyway and just 2 more DOF should be considered for including sinkage and trim, this is less straightforward now and leads to a combination of given and predicted motions.

#### 2.3.2 Analysis of predicted forces

The analysis of the predicted time histories of the longitudinal and transverse forces  $X$ ,  $Y$  and the roll and yaw moments  $K$ ,  $N$  is the same as when performing PMM or CPMC model tests. Moreover, since no artificial time lag between predicted forces and prescribed motions arise and no inertial forces have to be subtracted (no filters, no swinging masses), the analysis is easier than performing model tests.

Similar to when performing model tests there are different ways of determining the manoeuvring derivatives and the “virtual” test program has to be decided according to this and to the used mathematical model (e.g. the derivatives to be determined).

### 3. SIGNIFICANT PARAMETERS

The first step of any numerical investigation for manoeuvring consists in analysing the considered case and taking decisions like limiting the calculations to double body flow or taking the free water surface into account, considering the free sinkage and trim or not, performing the simulations for the ship model or for the full scale ship. This is followed by the proper choice of a turbulence model, discretisation schemes,

grid and time resolution, and the choice of the boundary conditions at the borders of the grid.

In addition, several parameters of the used code have usually to be chosen as well, for instance: the number of (outer) iterations within each time step, the number of (inner) iterations within an outer iteration, values for diverse under-relaxation factors, among others. Depending on the code, other settings could also be required and have a strong influence on the result of the computations. For these reasons, experience in viscous flow computations and insight about the RANS code going to be used are prerequisites for successful CFD based manoeuvring prediction.

## 4. EXAMPLES

### 4.1 Direct Manoeuvring Simulation

High requirements on the used code as well as to the level of expertise and large computational capability are required in order to carry out direct manoeuvring simulations. The method is getting more common and based on validation between calculations and free running model tests the results based on direct simulations looks promising. Examples may be seen in e.g. Broglia et al. (2011) where RANS simulations were performed for a free running twin screw tanker model performing turning circles and 20/20 zigzag. The propeller was modelled using a momentum disk approach where also the side forces were accounted for. Another example is Carrica et al. (2013), who did standard manoeuvres with at surface combatant at both model and full scale. Their results showed reasonable agreement with benchmark data, but they had issues regarding adequate modelling of propellers with side forces. As mentioned in section 2.1.4 the choice of propeller model should be considered carefully as it may have a signifi-

cant effect on the manoeuvring simulation results. More examples may be seen in the proceedings of the workshop SIMMAN 2014.

### 4.2 Simulation Based on Derivatives

The technique outlined above is applied here to predict the manoeuvrability of a Very Large Crude Carrier (VLCC), namely the tanker KVLCC1, used as a benchmark test in SIMMAN'08. Due to the low Froude number of the considered tanker and because negligible heel angles are expected during its manoeuvres all RANS simulations are performed without taking the water free surface into account.

Table 1 Main particulars of KVLCC2

$L_{pp}$	320.0 m
$B$	58.0 m
$T$	20.8 m
$\nabla$	312738 m <sup>3</sup>
$C_B$	0.8101
$L_{CB}$	3.48 %
GM	5.71 m
$i_{xx}/B$	0.375
$i_{zz}/L_{pp}$	0.25
Rudder lateral area	136.7 m <sup>2</sup>
Rudder helm rate	2.34 °/s
Ship speed $U_0$	15.5 kn

A RANS code is used to calculate the flow around the tanker at several static conditions and during virtual pure surge, pure sway, pure yaw and combined sway-yaw tests to obtain a rather simple set of hydrodynamic coefficients of Abkowitz type, see below.

All dynamic tests are simulated using the same multi-block structured grid with about one million cells with (some) non-matching block interfaces. The semi-balanced horn rudder, embedded in an individual grid box, is not deflected during these simulations. For static cases with deflected rudder and constant drift angle and/or

yaw rate only this grid box is replaced by another according to the considered rudder angle.

The grid dependency of the results has to be checked at least by means of selected calculations on different grids. In the present case the values of all forces and moments acting on the ship obtained on coarse, medium and fine grids behaved consistently and differed less than 10% from each other. Although this check cannot replace a real Uncertainty Analysis (UA) it may be a good compromise in practise.

The computations are performed on a ship fixed grid using a Cartesian non-inertial coordinate system. The standard two equations  $k-\omega$  turbulence model with wall functions is used. During dynamic tests the motions are imposed through the boundary conditions and corresponding inertial forces added to the RANS equations, see Cura and Vogt (2002).

The needed CPU time for simulating dynamic tests amounts nowadays still several days per period on a single processor of a normal PC but can be much less if a parallel code is run on a cluster with hundreds of processors. The static tests usually take some few hours depending on grid resolution.

Vortex lattice data for the propeller of a typical tanker was used in the present case. The rate of revolutions was set so that the resulting thrust balanced the resistance computed during a steady straight ahead motion of the model (model self propulsion point). This rate was kept constant throughout the computations.

Fig.4 shows the velocity distribution just behind the propeller plane during a simulated combined sway-yaw test at a certain time when the ship is turning to starboard. The white circle indicates the body force region.

In order to obtain all manoeuvring derivatives except those depending on the rudder angle and surge velocity, five dynamic tests with large velocity amplitudes and a common non-dimensional period  $T' = TU_0/L_{pp} = 3.369$  (20 seconds in model scale) are simulated.

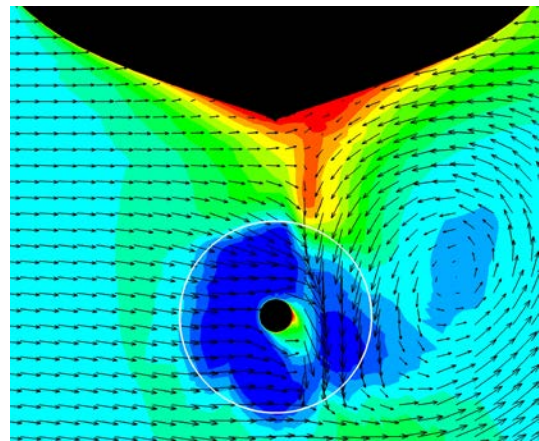


Fig.4 Snapshot of the velocity field behind the propeller during a simulated sway-yaw test

Similar to real tests, the non-dimensional amplitudes of the harmonic motions should be chosen so that they cover the expected range of the motion parameters during the manoeuvres.

In the present example the amplitudes were:  $u' = u/U_0 = 0.10$  for pure surge,  $v' = v/U_0 = 0.35$  for pure sway,  $r' = rL_{pp}/U_0 = 0.70$  for pure yaw and  $-0.35, 0.20$  and  $-0.20, 0.40$  for two combined sway-yaw tests, respectively.

The RANS simulations were done for the tanker's model (scale 1:45.7) at a speed of 1.179 m/s. The time step chosen for the RANS simulation corresponded to 1/2500 of the motion period in all cases.

The hydrodynamic forces and moments acting on the ship are obtained by integrating the pressure and shear stresses on the hull and appendages. The predicted time histories during simulated pure sway, pure yaw, as well as com-

bined sway- yaw can be seen in Fig.5. The longitudinal force  $X'$ , side force  $Y'$  and yaw moment  $N'$  have been made non-dimensional with water density, ship speed, length and draught.

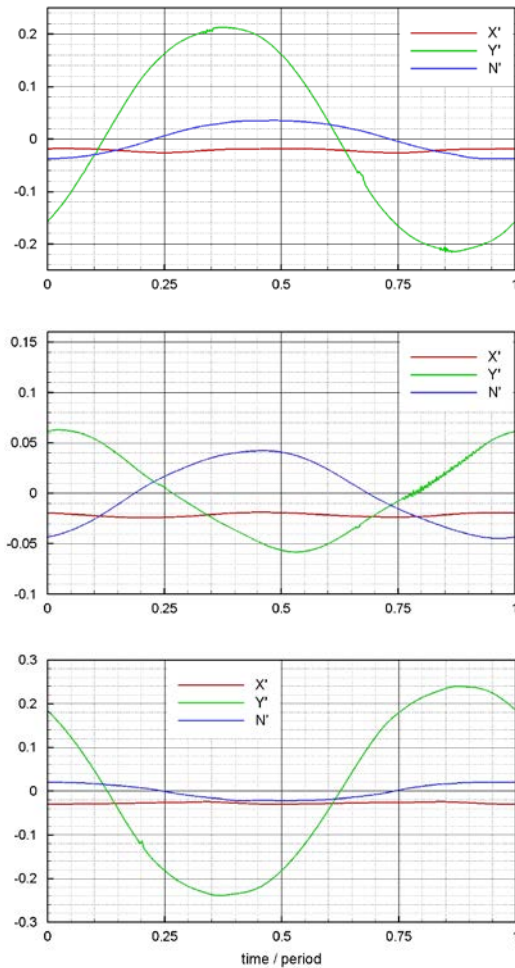


Fig.5 Forces and yaw moment during one period of a virtual pure sway and pure yaw test and a combined sway-yaw test (top to bottom)

Rudder angle depending manoeuvring derivatives can be determined by computing rudder angle tests at several drift angles and yaw rates resulting in a total of 42 cases.

Fig.6 shows the stern arrangement of the virtual model of KVLCC1 with the rudder deflected 35° to starboard. The pressure field on the rudder computed for steady straight ahead

motion is influenced by the effect of the propeller, rotating to the right over the top. Negative pressure regions are depicted in blue, while positive pressure regions are in red.

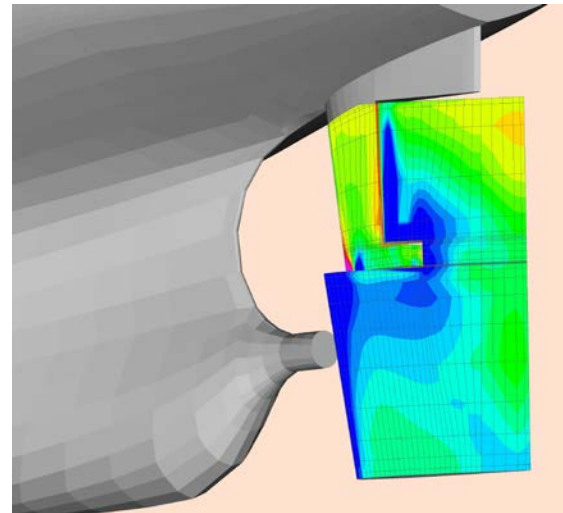


Fig.6 Stern arrangement of the virtual ship model and computed pressure on the rudder deflected 35°

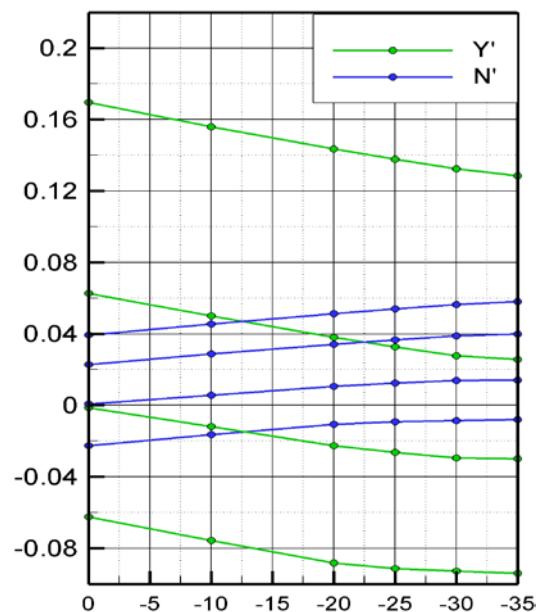


Fig.7 Computed non-dimensional side force and yaw moment during rudder angle tests at drift angle - 10°, 0°, 10° and 20°

The computed non-dimensional side force and yaw moment acting on the hull for all static

cases are summarised in Fig.7 and Fig.8 for oblique towing and steady turning conditions respectively.

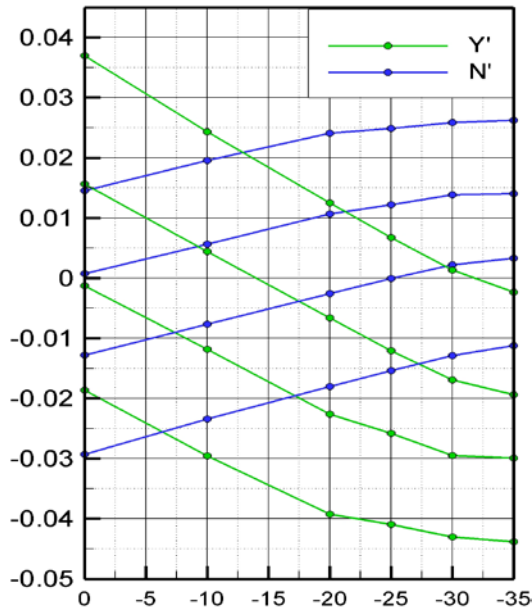


Fig.8 Computed non-dimensional side force and yaw moment during rudder angle tests at non-dimensional yaw rate -0.25, 0, 0.25 and 0.50

The time histories of the forces obtained from the RANS simulations for the 5 dynamic tests described above are used to determine the coefficients of the mathematical model in the same way as if PMM tests would have been done. This yields the coefficients in rows 4-18 of Table 2.

Regression analysis of the data obtained from static cases with deflected rudder yields the coefficients depending on the rudder angle written in rows 1-3 and 19-23 in Table 2.

The hydrodynamic coefficients shown in Table 2 have been made non-dimensional with water density, ship speed and length and multiplied by 1000, and are used to simulate standard rudder manoeuvres according to IMO (2002). For this purpose the motion equations of the ship in four degrees of freedom (4 DOF) were used.

However, the dependency of the non-dimensional magnitudes  $X'$ ,  $Y'$ ,  $N'$  and roll moment  $K'$  (not shown) on heel angle and roll rate was neglected since no significant roll motion was expected for the considered tanker. The sub-indices  $u$ ,  $v$ ,  $r$  and  $\delta$  denote the surge, sway and yaw velocities and the rudder angle, respectively.

Table 2 Manoeuvring Derivatives

0	$X'_o$	0	$Y'_o$	0	$N'_o$	0
1	$X'_\delta$	0	$Y'_\delta$	4.44	$N'_\delta$	-2.06
2	$X'_{\delta\delta}$	-2.09	$Y'_{\delta\delta}$	-0.24	$N'_{\delta\delta}$	0.16
3	$X'_{\delta\delta\delta}$	0	$Y'_{\delta\delta\delta}$	-2.95	$N'_{\delta\delta\delta}$	1.38
4	$X'_u$	-2.20	$Y'_u$		$N'_u$	
5	$X'_{uu}$	1.50	$Y'_{uu}$		$N'_{uu}$	
6	$X'_{uuu}$	0	$Y'_{uuu}$		$N'_{uuu}$	
7	$X'_\dot{u}$	-1.47	$Y'_\dot{u}$		$N'_\dot{u}$	
8	$X'_v$	0.11	$Y'_v$	-24.1	$N'_v$	-7.94
9	$X'_{vv}$	2.74	$Y'_{vv}$	2.23	$N'_{vv}$	-1.15
10	$X'_{vvv}$	0	$Y'_{vvv}$	-74.7	$N'_{vvv}$	2.79
11	$X'_\dot{v}$		$Y'_\dot{v}$	-16.4	$N'_\dot{v}$	-0.47
12	$X'_r$	-0.07	$Y'_r$	4.24	$N'_r$	-3.32
13	$X'_{rr}$	0.58	$Y'_{rr}$	0.56	$N'_{rr}$	-0.27
14	$X'_{rrr}$	0	$Y'_{rrr}$	2.58	$N'_{rrr}$	-1.25
15	$X'_\dot{r}$		$Y'_\dot{r}$	-0.46	$N'_\dot{r}$	-0.75
16	$X'_{vr}$	13.1	$Y'_{vr}$		$N'_{vr}$	
17	$X'_{vrr}$		$Y'_{vrr}$	-40.3	$N'_{vrr}$	8.08
18	$X'_{vvr}$		$Y'_{vvr}$	-9.90	$N'_{vvr}$	-3.37
19	$X'_{u\delta}$		$Y'_{u\delta}$	-4.56	$N'_{u\delta}$	2.32
20	$X'_{v\delta\delta}$		$Y'_{v\delta\delta}$	5.15	$N'_{v\delta\delta}$	-1.17
21	$X'_{vv\delta}$		$Y'_{vv\delta}$	7.40	$N'_{vv\delta}$	-3.41
22	$X'_{r\delta\delta}$		$Y'_{r\delta\delta}$	-0.51	$N'_{r\delta\delta}$	-0.58
23	$X'_{rr\delta}$		$Y'_{rr\delta}$	-0.98	$N'_{rr\delta}$	0.43

The main results of the simulated  $10^\circ/10^\circ$  zigzag test starting to starboard are compared with experimental results in Fig.9 which shows the heading angle  $\psi$  and the rudder angle  $\delta$  versus time. The 2<sup>nd</sup> overshoot angle predicted for KVLCC1 is slightly larger than measured and the overall agreement deteriorates with increasing time. However the characteristic parameters used to judge yaw checking and initial turning ability are predicted well, Table 3.

Table 3 Characteristic parameters of  $10^\circ/10^\circ$  test

$10^\circ/10^\circ$	SIM	EXP
time to attain	67 s	69 s
$x_{90^\circ}$	1.66 $L_{pp}$	1.73 $L_{pp}$
$\alpha_{01}$ [°]	8.1°	8.2°
$\alpha_{02}$ [°]	21.4°	19.4°
$r_{max}$	0.42 °/s	0.40 °/s

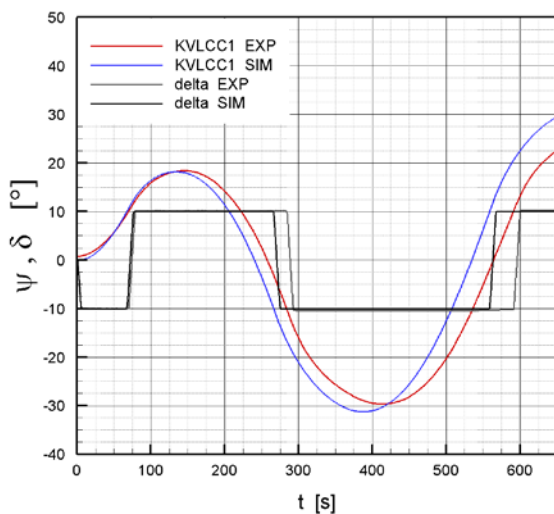


Fig.9  $10^\circ/10^\circ$  zigzag test starting to starboard

Any other rudder manoeuvre of interest can be predicted as well. For instance, the result of a

simulated turning circle to starboard with a rudder angle of  $35^\circ$  is compared with a free model test in Fig.10. The main parameters of the turning circle tests are compared in Table 4 with experiments showing good agreement. Note that the tanker fulfils the IMO recommendations with margin.

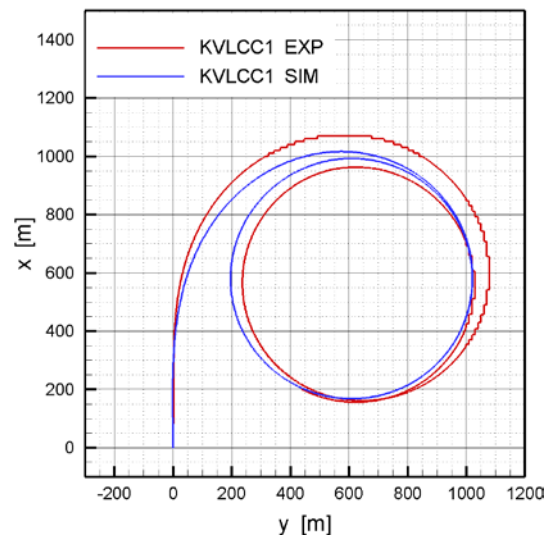


Fig.10 Turning circle test with  $\delta = 35^\circ$

Table 4 Characteristic parameters of turning circle test

$\delta = -35^\circ$	SIM	EXP
$x_{90^\circ} / L_{pp}$	3.10	3.03
$y_{180^\circ} / L_{pp}$	3.13	3.25
$\phi_{st} / L_{pp}$	2.58	2.44
$V_{st} / V_0$	0.39	0.37
$r_{st}$ [°/s]	0.43	0.42

This approach has become quite common when analyzing manoeuvrability using CFD. At SIM-MAN 2014 many institutes were seen to use this approach with good results.

## 5. REFERENCES

- Abdel-Maksoud M., Müller V., Xing T., Toxopeus S., Stern F., Petterson K., Tormalm M., Kim S., Aram S., Gietz U., Schiller P. and Rung T. (2015), "Experimental and Numerical Investigations on Flow Characteristics of the KVLCC2 at 30° Drift Angle", 5<sup>th</sup> World Maritime Conference, Rhode Island, USA.
- Abkowitz, M.A., (1964), "Lectures on Ship Hydrodynamics - Steering and Manoeuvrability", HyA Report HY-5, Copenhagen
- Anderson, D.A, Tannehill, J.C., Pletcher, R.H. (1984), "Computational fluid mechanics and heat transfer", Hemisphere, New York
- Blazek, J. (2001), "Computational Fluid Dynamics: Principles and Applications", Elsevier
- Brogliola, R., Durante, D., Dubbioso G. and Di Mascio, A. (2011), "Tuning Ability Characteristics Study of a Twin Screw Vessel by CFD", International Conference on Computational Methods in Marine Engineering, Lisbon, Portugal
- Carrica, P.M., Ismail, F., Hyman, M., Bhushan, S., and Stern, F. (2013), "Turn and Zigzag Maneuvers of a Surface Combatant Using a URANS approach with Dynamic Overset Grids", Journal of Marine Science and Technology, Vol. 18, No. 2, pp. 166-181
- Carrica, P., and Stern, F. (2008), "DES simulations of KVLCC1 in turn and zigzag manoeuvring with moving propeller and rudder", Proceedings SIMMAN 2008, Copenhagen
- Cebeci, T., Shao, J.R., Kafyeke, F., Laurendeau, E. (2005), "Computational Fluid Dynamics for Engineers", Horizons Publishing
- Cura Hochbaum, A. (2006), "Virtual PMM Tests for Manoeuvring Prediction", 26<sup>th</sup> ONR Symposium on Naval Hydrodynamics, Rome
- Cura Hochbaum, A., Vogt, M., Gatchell, S. (2008), "Manoeuvring prediction for two tankers based on RANS calculations", Proceedings SIMMAN 2008, Copenhagen
- Durante D., Brogliola R. Muscari, R. and Di Mascio A., (2010), "Numerical Simulations of a Turning Circle Manoeuvre for a Fully Appended Hull", 28<sup>th</sup> ONR Symposium on Naval Hydrodynamics, Pasadena, Los Angeles, USA.
- IMO, International Maritime Organization, (2002), Resolution MSC.137(76), "Standards for Ship Manoeuvrability", London
- Ferziger, J.H., Peric, M. (2002), "Computational Methods for Fluid Dynamics", Springer
- Hirsch C. (1988), "Numerical computation of internal & external flows", Wiley Series in Numerical Methods in Engineering
- Hirt, C.W., and Nichols, B.D. (1981), "Volume of Fluid (VOF) Method for the Dynamics of free Boundaries", J. of Comp. Physics, Vol.39
- L. Ji, K. Sreenivas, D. G. Hyams, R.V. Wilson (2010), "A Parallel Universal Mesh Deformation Scheme for Hydrodynamic Applications", 28<sup>th</sup> ONR Symposium on Naval Hydrodynamics, Pasadena, Los Angeles, USA.
- Launder, B.E., Reece, G.J. and Rodi, W. (1975), "Progress in the Development of a Reynolds-Stress Turbulent Closure.", Journal of Fluid Mechanics, Vol. 68(3), pp. 537-566.



# ITTC – Recommended Procedures and Guidelines

7.5-03  
04 - 01  
Page 17 of 17

## Guideline on Use of RANS Tools for Manoeuvring Prediction

Effective Date  
2017

Revision  
01

Launder, B.E., and Spalding, D.B. (1974), "The numerical computation of turbulent flows", Comput. Meth. in Appl. Mech. Eng. Vol.3

Menter, F.R. (1994), "Two-Equation Eddy-Viscosity Turbulence Models for Engineering Applications", AIAA Journal, Vol.32, No.8

Menter F.R., Kuntz M., and Langtry R., (2003), "Ten Years of Industrial Experience with the SST Turbulence Model", Turbulence, Heat and Mass Transfer 4, ed: K. Hanjalic, Y. Nagano and M Tummers, Begell House, Inc., pp. 625-632.

Muscari, R., R. Broglia and A. Di Mascio, (2008), "Trajectory Prediction of a Self Propeller Hull by Unsteady RANS Computations", 27<sup>th</sup> ONR Symposium on Naval Hydrodynamics, Seoul.

Osher, S., and Sethian, J.A. (1988), "Fronts Propagating with Curvature-Dependent Speed: Algorithms Based on Hamilton-Jacobi Formulations", J. of Comp. Physics, Vol.79

Sadat-Hosseini, H., Wu, P.C. and Stern, F. (2014), "CFD simulations of KVLCC2 maneuvering with different propeller modeling", Proceedings SIMMAN 2014, Copenhagen

Thompson, J.F., Warsi, Z.U.A., Mastin, C.W. (1985), "Numerical Grid Generation: Foundations and Applications", NorthHolland, New York

Wilcox, D.C. (1993), "Turbulence Modeling for CFD", DCW Industries, La Cañada, California